Journal of Power Sources 207 (2012) 160–165

Contents lists available at SciVerse ScienceDirect

Journal of Power Sources

journal homepage: www.elsevier.com/locate/jpowsour

Facile synthesis of β-Li_3VF_6: A new electrochemically active lithium insertion material

Anna Basa[a], Elena Gonzalo[b], Alois Kuhn[b], Flaviano García-Alvarado[b,*]

[a] Institute of Chemistry, University of Białystok, Hurtowa St. 1, 15-399 Białystok, Poland
[b] Universidad San Pablo-CEU, Departamento de Química, Urbanización Montepríncipe, 28668 Boadilla del Monte, Madrid, Spain

ARTICLE INFO

Article history:
Received 20 December 2011
Received in revised form 24 January 2012
Accepted 27 January 2012
Available online 6 February 2012

Keywords:
Lithium vanadium fluoride
Nanoparticles
Lithium batteries
Electrode material
Electrochemical behavior
Ball milling

ABSTRACT

The β-modification of Li_3VF_6 is easily prepared following a precipitation reaction at moderate temperature avoiding the high temperature route normally used for preparing related fluorides. Precipitation conditions for Li_3VF_6 have been optimized for two different alcohols to obtain better electrochemical performances. Temperature has been found to play an important role in the progress of precipitation reaction and in the phase purity of the resulting product. Best results were achieved for 2-propanol based solutions at 60 °C and for ethanol based solutions at 45 °C containing VCl_3, $HF_{(aq)}$ and Li_2CO_3 as starting compounds. In both cases large agglomerates, though of different size and shape, are obtained. These are composed of smaller particles of 20–30 nm. Electrochemical performances of as prepared Li_3VF_6 materials as electrode in lithium rechargeable batteries are modest with a maximum capacity of only 30 mAh g^{-1}. However, processing these materials by ball milling with carbon allows the capacity to increase to its theoretical value, 144 mAh g^{-1}, accordingly to the complete reduction of V^{3+} to V^{2+}. The observed average reduction potential for V^{3+} to V^{2+}, 2 V, may be certainly higher than that found in oxides but not high enough to be considered for application as the positive electrode. However, Li_3VF_6 is then another example of the β-Li_3MF_6 type-structure hosting lithium through an electrochemical insertion reaction. On the other hand, reversible oxidation of V^{3+} through lithium de-insertion, which would lead to the formation of $Li_{3-x}VF_6$ phases has not been successful yet. Taking into account the redox intercalation chemistry of vanadium in oxides, the reversible reduction of V^{3+} to V^{2+} and the irreversible oxidation of V^{3+} to V^{4+} in the herein presented fluoride make a significant difference derived from the nature of the non metal X. Then, research of fluorides is a path to find new chemistries for lithium batteries.

1. Introduction

Increase of energy of present batteries can only be achieved by using cathodes with higher redox potentials or higher capacity. Research of new structures containing the well known high or low redox potential couples Ni^{3+}/Ni^{4+}, Co^{3+}/Co^{4+}, Ti^{4+}/Ti^{3+}, etc. is the most common approach to innovative oxide materials with improved capacity, reversibility, etc. [1–10]. On the other hand, increase of the redox potential of a given metal couple has been attained by means of the inductive effect displayed on the M—O bond. This has been successfully applied to the development of phosphate and silicate based cathodes and other polioxoanionic materials [11–13]. However, significant increase of the redox potential can be also achieved for a given metal by increasing the ionicity of the M—X bond. In this connection it is well known that the high ionicity of the M—F bond produces a high redox potential of the respective transition metal [14,15]. Thus, the operating voltage of batteries using transition metal fluorides as the cathode is expected to be higher than that for homologous oxides for the same metal redox couple. Accordingly, high specific energies have been already reported for several binary metal fluorides [14].

Ternary metal fluorides are also interesting from an electrochemical point of view and recent reports described their use as electrodes for sodium batteries [16,17]. In this connection, we have recently reported on the electrochemical lithium insertion properties of new potential positive electrode materials in the Li–Fe–F system: the α- and β-polymorph of Li_3FeF_6 [18,19]. The α-polymorph (monoclinic) was found to be an advantageous material, in as much as it can be prepared by precipitation from aqueous solution at 25 °C. Particles with sizes ranging from 250 to 400 nm (and larger but always submicrometric), were obtained following the reported precipitation route [18]. Nevertheless, extended and reversible lithium insertion was not observed until the as prepared samples were mechanically milled with carbon. The original particle size (ca. 250–400 nm) was reduced to ca. 50 nm after milling α-Li_3FeF_6 with carbon for 12 h and 70% of theoretical quantity of lithium could be inserted after this processing accompanied by the partial reduction of Fe^{3+} to Fe^{2+}. A modified synthesis method

* Corresponding author. Tel.: +34 91 3724728; fax: +34 91 351 0475.
E-mail address: flaga@ceu.es (F. García-Alvarado).

0378-7753/$ – see front matter © 2012 Elsevier B.V. All rights reserved.
doi:10.1016/j.jpowsour.2012.01.148

to Li_3FeF_6 involving precipitation with ethanol has been recently described [20]. However, in that work no further details were given whether the synthesis conditions used by the authors produced nanocrystals suitable for lithium insertion without further need of reduction of particle size by extended milling, coating with carbon, etc. More recently the full capacity of α-Li_3FeF_6, 140 mAh g^{-1} was achieved for samples precipitated at 0 °C and using mixtures of water and 2-propanol as precipitation media [21]. Though 20 nm particles were formed upon precipitation, these were agglomerated in a raspberry-like morphology (200 nm diameter). Finally, breaking the large agglomerates and providing a proper mixing with carbon by ball milling, enabled the intercalation in the 20 nm particles to reach the full capacity corresponding to the complete reduction of 1 Fe^{3+} to Fe^{2+}.

Note that the high ionic nature of the M—F bond is clearly advantageous to produce high energy cathode materials, but one of the drawbacks is that most of these fluorides are insulators. This problem has been overcome at present for other cathode materials as for the commercialized $LiFePO_4$ electrode. Several authors proved that some of the paths followed to overcome the limitations encountered for $LiFePO_4$ can be effectively applied with success to fluorides [16–18,22,23]. On the other hand, we have recently shown that proper optimization of the synthesis procedure, did not only enable intercalation in insulating fluorides but also allowed the theoretical capacity to be reached at acceptable current rates [21]. These results encouraged us to search for other ternary fluorides to gain knowledge on the intercalation abilities of these materials that have received limited attention in the past decades.

It is now even clearer that synthesis procedures are key factors to be investigated in order to find new intercalation materials opening a path to new electrode materials for lithium rechargeable batteries. The present work addresses this new topic through the investigation of synthesis conditions and electrochemical properties of another compound of the Li_3MF_6 family related to Li_3FeF_6. We herein present the preparation of nano-Li_3VF_6 and its ability to intercalate 1 Li/formula at 2 V delivering a capacity of 144 mAh g^{-1}. Though the output potential is not high enough to be useful as a new cathode, the ability of Li_3VF_6 to intercalate lithium, paralleling Li_3FeF_6, is demonstrated. We are presently investigating other related transition metal fluorides that release a redox potential, high enough to be used as cathode in lithium batteries.

2. Experimental methods

2.1. Preparation

The synthesis route used is similar to that described for the monoclinic form, the α-polymorph, of Li_3FeF_6 [18,21], following a precipitation reaction in aqueous solution accordingly to the chemical equation:

$$VCl_3 + 6HF + (3/2)Li_2CO_3 \rightarrow Li_3VF_6 + (3/2)CO_2 + 3HCl + (3/2)H_2O \quad (1)$$

We used either 2-propanol or ethanol to precipitate the fluoride on the instant based on the successful results obtained previously for Li_3FeF_6 [21].

The complete procedure can then be summarized as follows: 2.619 g of VCl_3 dissolved in distilled water (typically 25 mL) was mixed with the stoichiometric quantity of an aqueous HF solution (40%). (Note that hydrofluoric acid is toxic and corrosive and must be handled with caution. Hence all operations were carried out in a laboratory fume hood and using protective gear to avoid contact and inhalation.) After adding Li_2CO_3 (stoichiometric amount) a transparent solution was obtained. This solution was then held at constant temperature (0 °C, 25 °C and 60 °C). The fluoride was precipitated by adding 75 mL of 2-propanol to the ca. 25 mL solution containing the solved fluoride. Though precipitation of a green powder started immediately, the solution was stirred for 5 min to promote multiple nucleation. The obtained powder was centrifuged, washed twice with small portions of 2-propanol and finally dried at 60 °C overnight in a drying oven. An identical procedure was used for ethanol, but working at 0 °C, 25 °C and 45 °C, respectively.

2.2. Structural and chemical characterization

Phase identification of as precipitated product and lithium intercalated compounds was made by X-ray diffraction using a X'Pert PRO PANalytical diffractometer operated at 45 kV and 40 mA, equipped with a hybrid monochromator, working with $CuK_{\alpha 1}$ (λ = 1.54056 Å) radiation and a Bruker AXS' LynxEye detector. The selected 2θ angular range was 4–75° with a 0.04°/10 s scan rate operated in continuous scan mode. Diffraction patterns were analyzed by full profile pattern matching [24] using the FullProf program [25].

Morphological characterization was carried out by means of Scanning Electron Microscopy (JEOL JSM-6335F and JEOL JSM-6400).

Samples were further characterized by thermal analysis to obtain information concerning stability. Samples were analyzed with a TGA/DTA Netzsch STA 409 apparatus by heating them at 10 K min^{-1} up to 600 °C under either air or flowing nitrogen (H_2O content ca. 2 ppm). XRD patterns of products after thermal treatment were recorded.

2.3. Mechanical milling

Reduction of particle size and mixing with carbon have been accomplished by grinding the as obtained products and conductive carbon with a planetary-type Pulverisette 7 ball mill (Fritsch GmbH, Germany). The following conditions were used for different dry milling times ranging from 1 to 12 h in air: sample weight, 1 g; grinding media, 2 balls with 10 mm diameter each; milling media and chamber material, zirconium dioxide; volume of grinding chamber, 20 mL; mill speed, 500 rpm.

2.4. Electrochemical characterization

Electrochemical cells were used to investigate the possible lithium insertion and de-insertion reaction of Li_3VF_6. Experiments were performed in CR2032 coin cells where a lithium foil was used as the negative electrode. For the positive electrode, either the as prepared powder, manually mixed with carbon, or the composite obtained by ball milling were conformed as pellets by uniaxial pressing. In all cases the electrode components were monoclinic Li_3VF_6, carbon black and a binder (PTFE) in a 72:25:3 weight ratio. A 1 M $LiPF_6$ solution in EC:DMC (1:1) was used as the electrolyte (commercial battery electrolyte LP30, SelectiLyte™). Cells were run using a MacPile II system. The electrochemical behavior of Li_3VF_6 composites was tested in galvanostatic mode, using a current density of 0.1 mA cm^{-2}. Potentiostatic experiments were run at 10 mV/0.5 h.

3. Results and discussion

Seeing that previous reports on Li_3FeF_6 indicated that the smallest particle size was obtained at low temperature (0 °C), using mixtures of water to 2-propanol ratio of 1:3 [18], these conditions were first used to precipitate Li_3VF_6 accordingly to Eq. (1). Contrarily to the results obtained for Li_3FeF_6 under these conditions

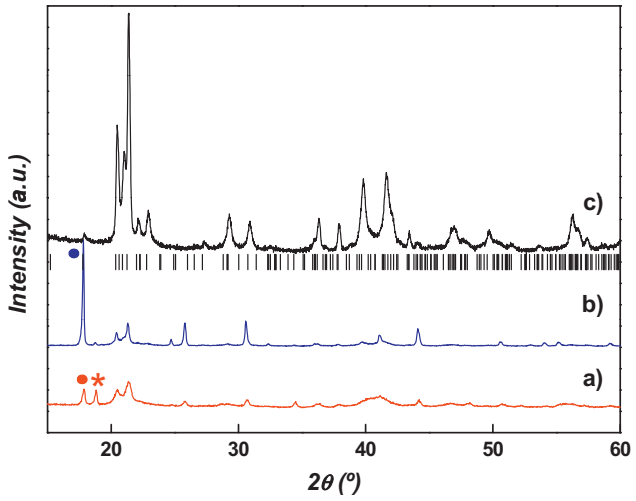

Fig. 1. X-ray diffraction patterns of samples with nominal composition Li_3VF_6 precipitated from aqueous solution using 2-propanol in a 1:3 w:2p ratio at 0 °C (a), 25 °C (b), and 60 °C (c). Vertical bars in (c) indicate the positions of the Bragg peaks of the phase β-Li_3VF_6 (S.G. C2/c). Marks on (a) and (b) correspond to the main diffraction peaks of different forms of $VF_3{\cdot}3H_2O$.

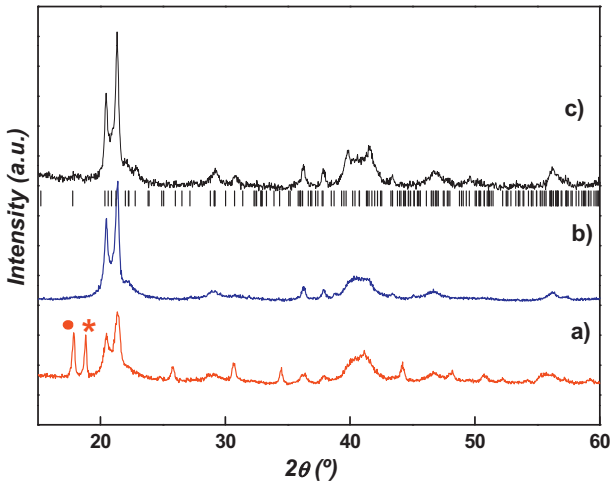

Fig. 3. X-ray diffraction patterns of samples with nominal composition Li_3VF_6 precipitated from aqueous solution using ethanol in a 1:3 w:2p ratio at 0 °C (a), 25 °C (b), and 45 °C (c). Vertical bars in (c) indicate the positions of the Bragg peaks of the phase β-Li_3VF_6 (S.G. C2/c). Marks on (a) correspond to the main diffraction peaks of different forms of $VF_3{\cdot}3H_2O$.

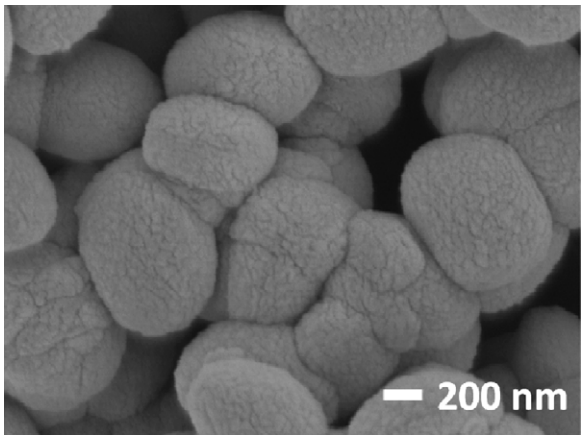

Fig. 2. Typical SEM image of β-Li_3VF_6 precipitated at 60 °C from a 1:3 water to 2-propanol solution.

the precipitation product mainly consisted of rhombohedral vanadiumfluoride trihydrate, $VF_3{\cdot}3H_2O$, space group R3m (PDF card 069571) [26], exhibiting its main diffraction line at $2\theta = 17.86°$ and its monoclinic form, space group C2, which was previously described for the analogous chromium compound, $CrF_3{\cdot}3H_2O$ (PDF card 170316) with its main diffraction line at $2\theta = 18.83°$ [27]. These two main peaks are labeled in Fig. 1a. Other additional diffraction lines could be assigned to monoclinic β-Li_3VF_6. At 25 °C one of the $VF_3{\cdot}3H_2O$ forms is stabilized and becomes the main phase of the mixture (see Fig. 1b). However, as precipitation temperature increased to 60 °C, single phase β-Li_3VF_6 was obtained as it can be seen in Fig. 1c for which every diffraction line can be assigned to β-Li_3VF_6. Refined lattice parameters for β-Li_3VF_6: $a = 14.3631(8)$ Å; $b = 8.7162(3)$ Å; $c = 10.0185(4)$ Å; $\beta_{mono} = 96.007(3)°$, space group C2/c, were in good agreement with those previously reported [28].

The scanning electron microscopy (SEM hereafter) image depicted in Fig. 2 reveals the morphology of Li_3VF_6 obtained at 60 °C. Particles of similar size, near to the micrometric range have been also reported for Li_3FeF_6 at the same precipitation temperature, and reduction of particle size down to ca. 200 nm was only possible by lowering the precipitation temperature to 0 °C. Even though these big particles are composed by the agglomeration of smaller particles, electrochemical Li insertion performances are known to be very dependent on the starting agglomerates size. Unfortunately, decreasing temperature using 2-propanol as precipitation agent always leads to the formation of $VF_3{\cdot}3H_2O$. Then, we have tried another alcohol to reduce the synthesis temperature of β-Li_3VF_6.

Using water and ethanol in a 1:3 ratio at 0 °C the formation of rhombohedral and monoclinic $VF_3{\cdot}3H_2O$ is reduced when compared to the experiments performed with 2-propanol for the benefit of β-Li_3VF_6. At 0 °C the same mixture of phases obtained in the case of 2-propanol is observed (Fig. 3a). Single phase β-Li_3VF_6 is already obtained at 25 °C (Fig. 3b). Higher precipitation temperatures (up to 60 °C) did not vary the result regarding phase purity. As typical example of morphology and size a SEM image of a sample obtained by precipitation using a 1:3 water to ethanol ratio at 45 °C is shown in Fig. 4. It shows spherical raspberry-like agglomerates of ca. 450 nm, which are similar to those found for α-Li_3FeF_6 [21]. However, the size of agglomerates of α-Li_3FeF_6, precipitated at 0 °C (ca. 200 nm), was smaller than that of the present Li_3VF_6 (ca. 500 nm), which cannot be precipitated at such temperature due to the formation of $VF_3{\cdot}3H_2O$ as secondary phase. It can also be seen in the magnification shown in Fig. 4b that the agglomerates are composed by particles in the 20–30 nm range as it was also the case of α-Li_3FeF_6 [21].

Thermogravimetric analysis of β-Li_3VF_6 (not shown) indicates that this fluoride hydrolyzes above 150 °C. At 500 °C hydrolysis is complete in air while reaction is partial under nitrogen with small amount of water. It seems that β-Li_3VF_6 is more hydrolysable than α-Li_3FeF_6 for which hydrolysis was observed to occur above 200 °C under the same experimental conditions.

Li_3VF_6, precipitated from either 2-propanol (60 °C) or ethanol (45 °C), was used for electrochemical tests in Li cells. The first discharge of cells bearing as prepared β-Li_3VF_6 and two ball milled samples as the active component of the positive electrode down to 1.4 V are presented in Fig. 5. It can be seen that the initial discharge capacity of Li_3VF_6 obtained with ethanol (45 °C) is higher than that obtained with 2-propanol (60 °C), which agrees with the smaller size of agglomerates formed at lower temperature in ethanolic solution (see Figs. 2 and 4). After ball milling Li_3VF_6 with carbon for 5 h the discharge capacities of both samples still exhibit significant differences, while both samples are able to intercalate ca. 1 Li per formula unit after ball milling with carbon for 12 h. This

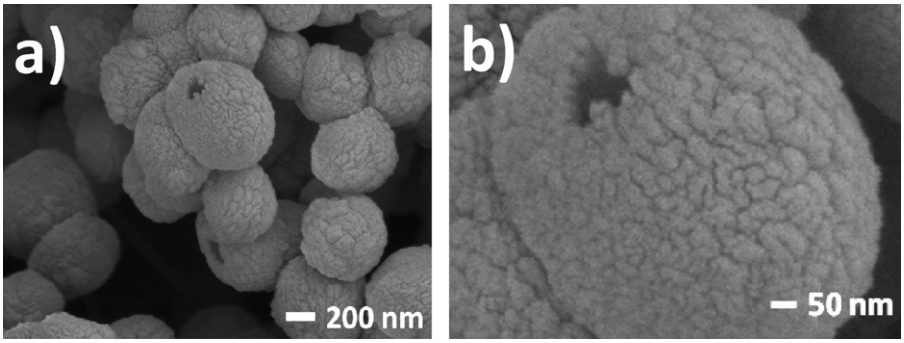

Fig. 4. Typical SEM image of β-Li_3VF_6 precipitated at 45 °C from a 1:3 water to ethanol solution (a) and a magnification showing a detail of an agglomerate (b).

corresponds to the theoretical capacity (144 mAh g^{-1} for the complete reduction of V^{3+} to V^{2+}). The improvement of capacity is in agreement with the observed reduction of the size of agglomerates as shown in Fig. 6 for β-Li_3VF_6 prepared by using a water and 2-propanol solution in a 1:3 ratio at 60 °C.

Fig. 7a shows the first discharge–charge cycle of a β-Li_3VF_6/Li cell. The active material corresponds to a sample precipitated in water and 2-propanol solution (1:3 ratio) at 60 °C which was afterwards ball milled with carbon for 12 h. The profile of both curves verifies the reversibility of the insertion reaction. However, the large polarization observed at high voltage points to a kinetic limitation of oxidation reaction. On the other hand, a significant loss of capacity is observed after the first discharge, while further cycling shows that capacity is well kept (see Fig. 7b) after the capacity loss of the first cycle. In any case, optimization of the electrode fabrication will be needed for decreasing such a capacity loss. On the other hand, reversible oxidation of V^{3+} to V^{4+} with Li de-insertion from β-Li_3VF_6 has not been achieved under our experimental conditions. It is worth mentioning that, a very recent patent claims

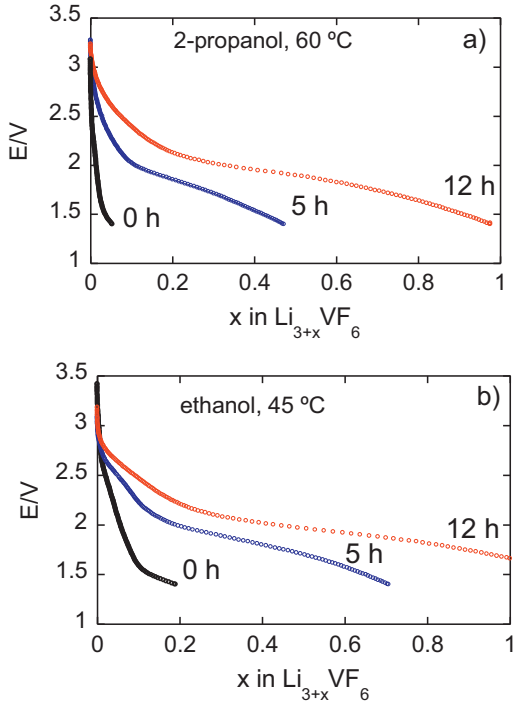

Fig. 5. First discharge curves of Li cells bearing β-Li_3VF_6 in the positive electrode obtained by precipitation from a 1:3 solution of water and 2-propanol at 60 °C (a) or ethanol at 45 °C (b). As prepared materials milled manually with carbon (0 h) and materials processed by ball milling with carbon (5 h or 12 h) are presented. Current density: 0.1 mA cm^{-2}.

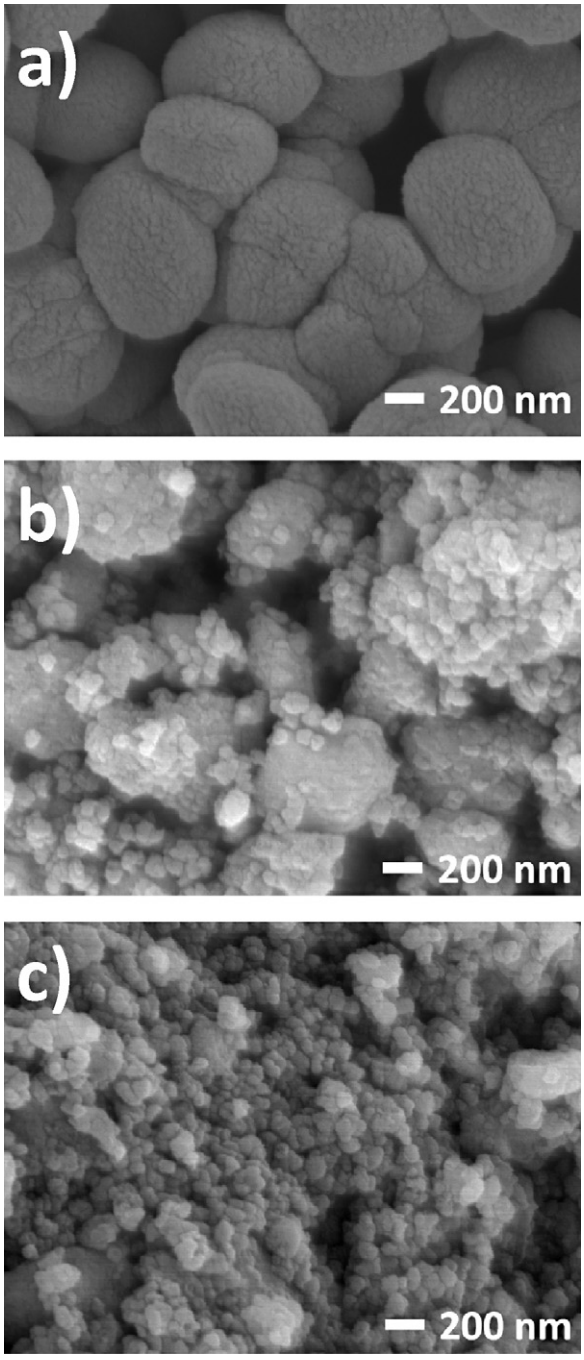

Fig. 6. SEM micrographs of β-Li_3VF_6 prepared using a water to 2-propanol ratio of 1:3 at 60 °C: as prepared (a), after 5 h (b) and 12 h (c) ball milling with carbon.

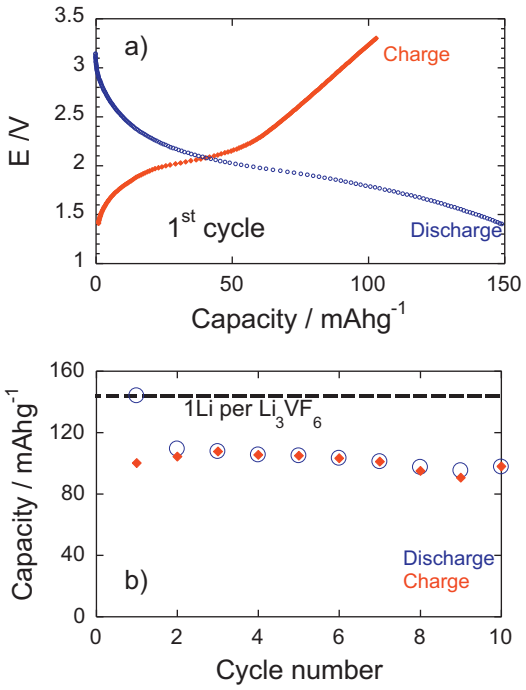

Fig. 7. (a) First discharge–charge cycle of a Li cell bearing as the positive electrode β-Li_3VF_6 milled for 12 h with carbon and (b) discharge (circles) and charge (diamonds) capacity on cycling for the same cell. Current density: 0.1 mA cm^{-2}.

that such oxidation is possible in the 4.3–4.5 V voltage range [29]. Unfortunately, no much more information can be extracted from the published document in as much as electrochemical curves are not included.

Interestingly, the equilibrium reduction potential for β-Li_3VF_6 was seen to be located at 2.0 V, as determined from discharge experiments performed under open circuit voltage conditions (not shown). This redox process is assumed to be due to $V^{3+} \rightarrow V^{2+}$ and is slightly higher than the value reported for the reduction of V^{3+} during Li insertion in $LiVPO_4F$ (1.8 V). These differences are explained with the higher inductive effect combined with increased ionicity exerted by the pure fluoride environment of vanadium in Li_3VF_6. Though the insertion voltage is not high enough to consider Li_3VF_6 useful as a positive electrode for lithium batteries, note that, the V^{3+}/V^{2+} redox couple has practically not been found in intercalation reactions of the most explored materials for lithium batteries, i.e. transition metal oxides, with the exception of recent reports of its use as the anode in aqueous lithium ion cells [30,31]. The most common redox couples regarding Li insertion in vanadium oxides are V^{5+}/V^{4+} (3.4–3.2 V) and V^{4+}/V^{3+} (2.9 V) for cathode applications [32–35]. Therefore, the result herein presented show that not only potential but also unusual redox couples may be found when different non metals are bonded to the transition metal. Thus, the thorough search of halides in general terms and especially fluorides or chlorides may open a new path to innovative materials for lithium batteries with new structure types.

4. Conclusions

The fluoride β-Li_3VF_6 has been obtained through a precipitation reaction at low temperature. This facile preparation route is advantageous toward the high temperature synthesis route normally used for related fluorides. The material exhibits the monoclinic β-Li_3MF_6 structure, which was recently shown as new host to lithium insertion. Precipitation conditions for β-Li_3VF_6 have been optimized for two different alcohols in order to obtain high purity samples with better electrochemical performances. Temperature was found to play an important role in the precipitation reaction and in the purity of the product. Best results were achieved for 2-propanol based solutions at 60 °C and for ethanol based solutions at 25–45 °C containing VCl_3, $HF_{(aq)}$ and Li_2CO_3 as starting compounds. Nearly micrometric agglomerates differing in size (from 500 to 900 nm) and shape are obtained in both cases. Agglomerates are composed of nanometric (20–30 nm) particles. Electrochemical performances of as prepared materials are poor and capacity was limited to 30 mAh g^{-1}. However, processing these materials by ball milling with carbon largely improves the capacity in as much as it allows the theoretical capacity, 144 mAh g^{-1}, to be delivered, accordingly with the complete reduction of V^{3+} to V^{2+}. The V^{3+}/V^{2+} redox couple displays an average reduction potential of 2 V, which is certainly higher than the same redox couple in oxides, but not high enough to be considered for application. Interestingly, Li_3VF_6 is presented as new example of the β-Li_3MF_6 type-structure hosting lithium through electrochemical reactions.

On the other hand, oxidation of V^{3+} to V^{4+}, i.e. the formation of lithium-deficient phases through Li de-insertion from Li_3VF_6 was not achieved under our experimental conditions. Taking into account the redox intercalation chemistry of vanadium oxides, the reversible reduction of V^{3+} to V^{2+} in conjunction with the irreversible oxidation of V^{3+} to V^{4+} in the herein presented fluoride makes a significant difference derived from the nature of the non metal, which points to a different path to find new chemistries for lithium batteries.

Acknowledgments

We thank Ministerio de Ciencia e Innovación and Comunidad de Madrid for funding the projects MAT2010-19837-C06-01 and S2009/PPQ-1626 respectively. Financial support from Universidad San Pablo CEU is also acknowledged and in particular the International Project Office. We also thank EADS-CASA and the Polish Ministry of Economy for funding the stay of A. Basa at San Pablo CEU University. We thank M.T Azcondo for TGA Analysis.

References

[1] K. Mizushima, P.C. Jones, P.J. Wiseman, J.B. Goodenough, Materials Research Bulletin 15 (1980) 783–789.
[2] J.R. Dahn, U. Vonsacken, C.A. Michal, Solid State Ionics 44 (1990) 87–97.
[3] H. Kawai, M. Nagata, M. Tabuchi, H. Tukamoto, A.R. West, Chemistry of Materials 10 (1998) 3266–3268.
[4] T. Ohzuku, A. Ueda, N. Yamamoto, Journal of the Electrochemical Society 142 (1995) 1431–1435.
[5] A. Kuhn, R. Amandi, F. Garcia-Alvarado, Journal of Power Sources 92 (2001) 221–227.
[6] A.R. West, H. Kawai, H. Kageyama, M. Tabuchi, M. Nagata, H. Tukamoto, Journal of Materials Chemistry 11 (2001) 1662–1670.
[7] K. Amine, H. Tukamoto, H. Yasuda, Y. Fujita, Journal of the Electrochemical Society 143 (1996) 1607–1613.
[8] C. Delmas, I. Saadoune, Solid State Ionics 53 (1992) 370–375.
[9] R. Kanno, T. Shirane, Y. Kawamoto, Y. Takeda, M. Takano, M. Ohashi, Y. Yamaguchi, Journal of the Electrochemical Society 143 (1996) 2435–2442.
[10] T. Ohzuku, A. Ueda, M. Nagayama, Y. Iwakoshi, H. Komori, Electrochimica Acta 38 (1993) 1159–1167.
[11] A.K. Padhi, K.S. Nanjundaswamy, J.B. Goodenough, Journal of the Electrochemical Society 144 (1997) 1188–1194.
[12] A. Nyten, A. Abouimrane, M. Armand, T. Gustafsson, J.O. Thomas, Electrochemistry Communications 7 (2005) 156–160.
[13] M.E. Arroyo-de Dompablo, U. Amador, F. Garcia-Alvarado, Journal of the Electrochemical Society 153 (2006) A673–A678.
[14] H. Arai, S. Okada, Y. Sakurai, J. Yamaki, Journal of Power Sources 68 (1997) 716–719.
[15] Y. Koyama, I. Tanaka, H. Adachi, Journal of the Electrochemical Society 147 (2000) 3633–3636.
[16] I.D. Gocheva, M. Nishijima, T. Doi, S. Okada, J. Yamaki, T. Nishida, Journal of Power Sources 187 (2009) 247–252.
[17] M. Nishijima, I.D. Gocheva, S. Okada, T. Doi, J. Yamaki, T. Nishida, Journal of Power Sources 190 (2009) 558–562.
[18] E. Gonzalo, A. Kuhn, F. Garcia-Alvarado, Journal of Power Sources 195 (2010) 4990–4996.

[19] E. Gonzalo, A. Kuhn, F. Garcia-Alvarado, Journal of the Electrochemical Society 157 (2010) A1002–A1006.
[20] I.D. Gocheva, Y. Kamimura, T. Doi, S. Okada, J. Yamaki, T. Nishida, Engineering Sciences Reports, Kyushu University 31 (2009) 7–11.
[21] A. Basa, E. Gonzalo, A. Kuhn, F. García-Alvarado, Journal of Power Sources 197 (2012) 260–266.
[22] P.N. Badway, F. Cosandey, G.G. Amatucci, Journal of the Electrochemical Society 150 (2003) A1209–A1218.
[23] G.G. Amatucci, Patent No.: US7371338B2 (2008).
[24] H.M. Rietveld, Acta Crystallographica 22 (1967) 151–152.
[25] J. Rodriguez Carvajal, Physica B 192 (1993) 55–69.
[26] D. Mootz, U. Schwarz, Acta Crystallographica Section C: Crystal Structure Communications 47 (1991) 1534–1535.
[27] Natl. Bur. Stand. (U.S.) Monogr. 25, Section 5 (1967).
[28] W. Massa, Zeitschrift Fur Kristallographie 153 (1980) 201–210.
[29] M. Schulz-Dobrik, M. Lerch, H. Ehrenberg, S. Nakhal, J. Koch, F. Scheiba, M. Herklotz, Electrode material and use thereof for production of electrochemical cells. Patent no. US 20110227001, USA (2011).
[30] Y. Xu, L. Zheng, Y. Xie, Dalton Transactions 39 (2010) 10729–10738.
[31] Y. Sun, S. Jiang, W. Bi, C. Wu, Y. Xie, Journal of Power Sources 196 (2011) 8644–8650.
[32] A. Tranchant, J.M. Blengino, J. Farcy, R. Messina, Journal of the Electrochemical Society 139 (1992) 1243–1248.
[33] L.A. Depicciotto, M.M. Thackeray, W.I.F. David, P.G. Bruce, J.B. Goodenough, Materials Research Bulletin 19 (1984) 1497–1506.
[34] L.A. Depicciotto, M.M. Thackeray, Solid State Ionics 18–19 (1986) 773–777.
[35] K. Ozawa, L.Z. Wang, H. Fujii, M. Eguchi, M. Hase, H. Yamaguchi, Journal of the Electrochemical Society 153 (2006) A117–A121.